Pergamon

0956-7151(95)00205-7

Acta mater. Vol. 44, No. 2, pp. 813–818, 1996
Elsevier Science Ltd

1359-6454/96 $15.00 + 0.00

MICROSTRUCTURE AND THERMAL CONDUCTION PROPERTIES OF Al_2O_3–Ag COMPOSITES

D. M. LIU[1] and W. H. TUAN[2]

[1]Materials Research Laboratories, Industrial Technology Research Institute, Chutung, Hsinchu 31015, Taiwan and [2]Institute of Materials Engineering, National Taiwan University, Taipei, Taiwan 10764, R.O. China

(Received 12 May 1994; in revised form 16 October 1994)

Abstract—Microstructure and thermal conduction properties involving thermal diffusivity and conductivity of composite, Al_2O_3–Ag, were investigated. The Ag particles observed in the composites were spread sporadically throughout the composite with inclusion size increasing with Ag content, rather than forming a network of thin film foil. Thermal conductivity of the composite increased with Ag content and followed composite theory prediction with a negligible influence of interfacial contact resistance. The temperature dependence of the thermal conductivity became less pronounced with increasing Ag content reflecting the nature of electron contribution in Ag rather than the typical phonon contribution in polycrystalline Al_2O_3. The lower composite conductivity at higher Ag contents as compared to theoretical predictions is due primarily to the residual pore phase, associated with the cavity formation for the composite containing 10 vol.% Ag.

1. INTRODUCTION

Brittle solids are susceptible to the scale of pre-existing flaws. However, a dominant methodology in improving the toughness of brittle solids is to fabricate composites. One of the important branches of composites is by incorporating the ductile metal particles [1–3], or fibers [4, 5] into the brittle solids, to produce cermet. This method illustrates a potential advantage in toughness improvement, especially in ceramic materials [6, 7], and has received attention theoretically and practically. One of the most promising features for cermets is the improved thermal-shock resistance. Morgan *et al.* [8] obtained good thermal shock characteristics in composites of Al_2O_3 matrix with small amounts (0.5–1.5 vol.%) of finely dispersed Pt or Cr metal. They reported that this thermal shock improvement is primarily due to the mechanical locking of ceramic grain by the metal inclusions, i.e. a crack bridging effect. The mechanism for such a toughness increment in brittle solids has been detailed in other publications [3, 5] and is beyond the scope of the present study.

This article deals mainly with the thermal conduction properties of the composite containing up to 10% Ag in an Al_2O_3 matrix, accompanied with microstructure characterization. Although the metal inclusions exhibit ductile characteristics, the large thermal expansion mismatch between the metal and ceramic may inevitably give rise to considerable internal stresses which may usually lead to internal fracture. A thermal cyclic flash-diffusivity method was thus employed to detect whether the internal fracture exists or not [9, 10].

2. EXPERIMENTAL PROCEDURES

A powder mixture consisting of Al_2O_3 (AKP-50, Sumitomo Chem. Co. Ltd, Japan) and Ag_2O (Johnson Matthey Co., U.K.) was ball-milled, with zirconia balls as media, in ethanol solution for 24 h. The slurry was dried with a rotary evaporator (N-1, Tokyo Rikakikai Co. Ltd), followed by die-pressing under an unidirectional pressure of 100 MPa. The as-pressed compacts were then sintered in air at 1500–1700°C for 1 h. The Al_2O_3 grain size and the inclusion size were determined on a polished surface by an image analyzer (Quantimet 520, Cambridge Co.). Specimens used for thermal conduction measurement were ultrasonically machined into disks with thickness $\sim$1.5 mm and diameter $\sim$10 mm. The detailed procedures for the determination of thermal diffusivity (α) and heat capacity (C_p) were reported in another paper [12]. The microstructure of the composite was examined using scanning electron microscopy (SEM, Cambridge Instruments, S-360).

3. RESULTS AND DISCUSSION

3.1. Microstructure evolution

The incorporated Ag_2O powder decomposed into metal silver and oxygen during the heating stage, and resulted in fine Ag particles as the second-phase inclusion in the Al_2O_3 matrix after sintering. The microstructure of the composite for a representative

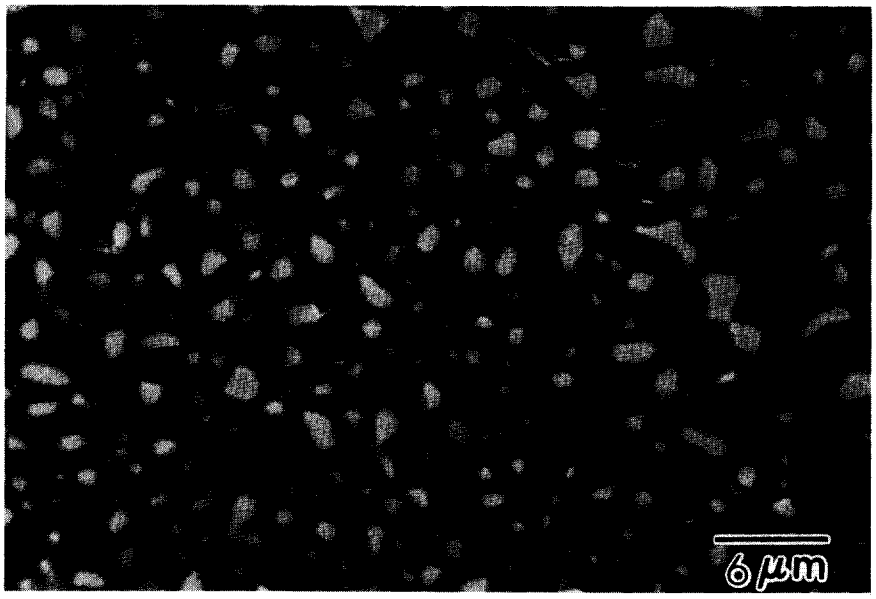

Fig. 1. Scanning electron micrograph, showing a polished surface of Al_2O_3–Ag composite (10 vol.% Ag) where the light regions denote the Ag inclusions and the dark regions are Al_2O_3 matrix.

specimen containing 10 vol.% Ag was illustrated in Fig. 1. The numerous light regions denote the Ag inclusions and the dark regions are Al_2O_3 matrix. Unlike the composites prepared by Morgan [13] over which a three-dimensional network of thin metal foil was formed in the brittle matrices, the Ag inclusion (melting point ~960°C) had a different morphology. With the exception of a few larger inclusions (~4 μm), the majority of the inclusions are small and are sporadically distributed throughout the solid. The size of the matrix grain and the inclusion was listed in Table 1 with various Ag contents. With increase of Ag content, Al_2O_3 grain size became smaller indicating that the grain boundary movement was strongly inhibited during sintering. However, the increase in inclusion size is believed to be due to the coalescence between agglomerates of small inclusions while treating at elevated temperatures [7].

One of the important features in ceramic matrix composites is the occurrence of internal fracture due to differential thermal contraction particularly for composites with brittle constituents [14]. This can always weaken the strength of the composites and subsequently limits their structural applications. However, some of the drawbacks may reduce upon the incorporation of ductile metal inclusion into brittle matrix, and a significant toughening improvement is frequently obtained [3, 7]. In the composite, the thermal expansion mismatch between Al_2O_3 ($\alpha_{Al_2O_3} = 8.8 \times 10^{-6}/°C$) and Ag ($\alpha_{Ag} = 10^{-6}/°C$) is large, i.e. $\Delta\alpha = 11.2 \times 10^{-6}/°C$. Since metal silver is extreme ductile, it is hypothesized that stress due to differential thermal contraction between Al_2O_3 and Ag can be released above a critical temperature, ΔT. Below such a temperature, the stresses arise and subsequently cause spontaneous microcracking. Moreover, the magnitude of the stresses increases with the third-power of the inclusion size [15]. The critical inclusion size (R_c) for spontaneous microcracking inside the composite can then be determined by a model recently proposed by Liu [16]. The model described that the stored strain energy in brittle composites is a strong function of both the content and size of second-phase inclusion, analogizing to that derived by Davidge and Green in terms of a strain energy criterion [14] by:

$$R_c \geqslant \frac{6\gamma_A}{2\sigma_\alpha^2/E_m[(F_r^2 + F_\theta^2) - 2\nu_m F_\theta(F_\theta + F_r)] + \sigma_\alpha^2(1-2\nu_d)^2/E_d} \quad (1)$$

where γ_A is fracture surface energy of matrix phase (assumed ~1.0 J/m² for Al_2O_3), σ_α is the internal residual stress, ν is the Poisson's ratio which is 0.37 for Ag and 0.257 for Al_2O_3, E is the Young's modulus, 380 GPa for Al_2O_3 and 71 GPa for Ag, and factors F_r and F_θ are functions of inclusion content. The subscripts m and d denote the matrix and inclusion phase, respectively. Figure 2 shows the resulting predicted curves for temperature difference ΔT of 500 and 600°C vs experimental observation (open circle). Obviously, spontaneous microcracking

Table 1. Porosity, inclusion size and Al_2O_3 grain size of Al_2O_3–Ag composite

Ag (vol.%)	Porosity (%)	Inclusion size (μm)	Al_2O_3 size (μm)
0	0.6	—	5.16
2.5	1.0	1.21	4.52
5	2.0	2.5	4.19
10	3.4	2.7	4.06

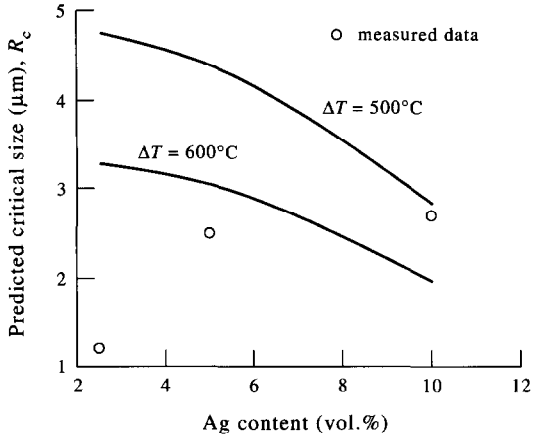

Fig. 2. Comparison made between the predicted critical Ag size under different ΔT and the measured inclusion size for various Ag contents.

would likely occur if the internal stresses were developed at ΔT approx. 500°C at 10 vol.% Ag. This is because the measured inclusion size, 2.7 μm, is roughly the same as the value derived theoretically under $\Delta T = 500$°C. Any increase in ΔT indicates that the stresses are readily developed at a higher temperature on cooling and this usually causes a reduction in Ag size required for the initiation of microcracking for a given inclusion content.

3.2. *Thermal conduction behavior*

As a dielectric solid, the thermal diffusivity of polycrystalline alumina exhibited is typical of phonon conduction behavior. By incorporation of metal silver the thermal diffusivity of the composites increases (Fig. 3), with increasing content of Ag. The thermal conductivity of the composite can be obtained by multiplying the thermal diffusivity, heat capacity (given in Table 2), and the bulk density of the composite, as shown in Fig. 4. The dimensional change due to thermal expansion at various temperatures was considered for accurate estimation. In-

Table 2. Heat capacity (J/g·K) of the Al_2O_3–Ag(x) composites at various temperatures (T). Data measured by using the laser-flash method as described in detail in Ref. [12]

x (%) / T (°C)	0	2.5	5	10
20	0.66	0.67	0.67	0.64
100	0.71	0.73	0.76	0.75
200	0.76	0.80	0.85	0.78
300	0.85	0.86	0.89	0.87
400	0.89	0.94	0.93	0.95
500	0.93	0.96	0.96	1.07
600	0.97	1.08	1.09	1.10

crease of the Ag content, the thermal conductivity of the composites increases and shows a weak temperature dependence, particularly at 10% Ag, resembling that observed in metal silver [17, 18]. This finding suggests that the electron contribution of the metal silver to the composite conductivity (at 10% Ag) is significant. Furthermore, this increase of composite conductivity reduces excessive heat accumulation and in certain conditions prevents the composites from thermally-induced fracture. Together with its improved fracture toughness [19], application of the composite in certain environments particularly when moderate thermal shock is required is encouraging.

Hasselman and Johnson [20] derived a series of expressions by modifying the original composite theories of Rayleigh [21] and Maxwell [22] to consider the effect of interfacial and thermal resistance. These expressions allow the effective conductivity of composite consisting of homogeneous matrix phase in which particles of second homogeneous phase are dispersed to be predicted. For spherical dispersions the equation is given by:

$$K_c = K_m \frac{\left[2\left(\frac{K_d}{K_m} - \frac{K_d}{ah} - 1\right)V_d + \frac{K_d}{K_m} + \frac{2K_d}{ah} + 2\right]}{\left[\left(1 - \frac{K_d}{K_m} + \frac{K_d}{ah}\right)V_d + \frac{K_d}{K_m} + \frac{2K_d}{ah} + 2\right]} \quad (2)$$

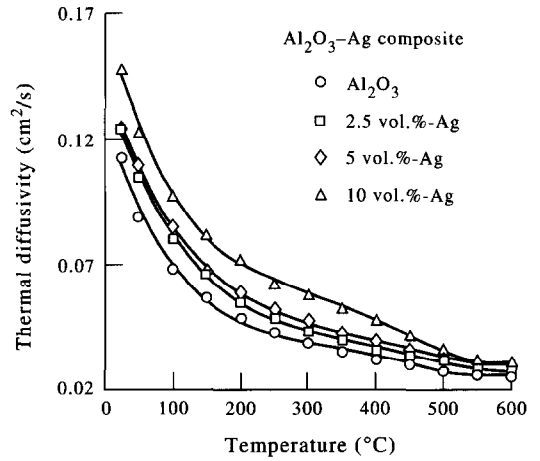

Fig. 3. Temperature-dependence of thermal diffusivity of Al_2O_3–Ag composite.

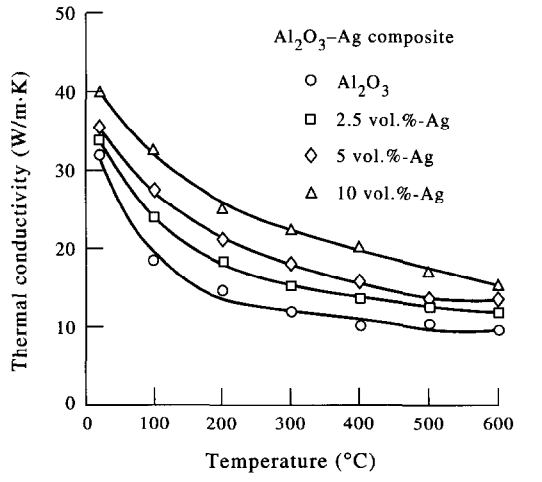

Fig. 4. Thermal conductivity of Al_2O_3–Ag composite.

where K_c is the effective thermal conductivity of composite, a is radius of sphere, h is interfacial thermal conduction coefficient, and V_d is the volume fraction of the dispersed phase. In the absence of interfacial thermal resistance, i.e. $1/h = 0$, equation (2) is identical to the original Rayleigh–Maxwell relation for K_c and is also consistent with Eucken's relation [23] for the case of a continuous phase with spherical inclusion.

By substituting the conductivity values of $Al_2O_3 = 32\ W/m \cdot K$ and $Ag = 410\ W/m \cdot K$ into equation (2) with various inclusion fractions, the calculated thermal conductivity line was attained as shown in Fig. 5 with the measured values denoted by circle symbols. The predicted conductivity is higher than the measured conductivity for Ag > 5%, which may arise from the pore phase and the probable microcracking effect aforementioned. However, the latter factor suggests $h = 0$ (valid for a complete separation of Ag/Al_2O_3 interface), and a value of 29.6 and 27.4 $W/m \cdot K$ is obtained using equation (2) and $h = 0$ for 5 and 10% Ag, respectively. These values are much smaller than the measured ones, indicating that the microcracking effect should be rather small if it does exist or may be absent.

Therefore, to determine the interfacial contact resistance ($1/h$) in equation (2) it is essential to further understand the Al_2O_3–Ag interface. Recently, Hasselman *et al.* [24] reported that in Al/SiC composites the composite conductivity increased sigmodially with increasing SiC particle size and reached a near-constant value for some critical inclusion diameter (D_c). Such a sigmodial change in thermal conductivity with particle size mainly results from increasing interfacial contact resistance and has been verified analytically by Benveniste and Miloh [25]. Above the critical diameter (D_c), the influence of the interfacial contact resistance on the K_c is negligibly small as compared to the contribution of inclusion phase to the overall composite conductivity [26]. In a recent communication by Liu [27], the h and corresponding a_c ($D_c = 2a_c$) can be determined by the following equations

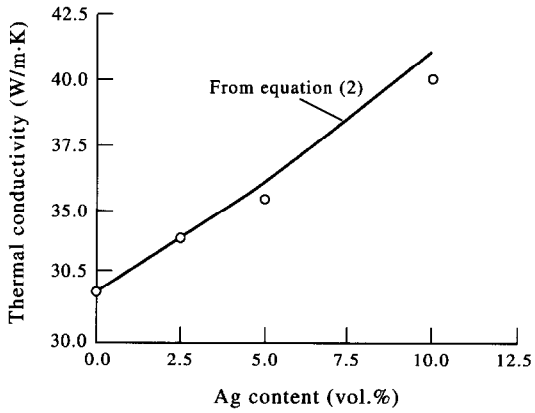

Fig. 5. Comparison of thermal conductivity made between theoretical prediction [equation (2)] and experimental observation in Al_2O_3–Ag composite.

Substituting $K_c = 39\ W/m \cdot K$ for 10% Ag, $a = 1.35\ \mu m$ ($D = 2.7\ \mu m$), and the known values of K_m and K_d into equation (3), the interfacial thermal conductance $h = 4.10 \times 10^8\ W/m^2 \cdot K$ is obtained. The critical size for a negligible interfacial resistance is then calculated to be $D_c = 2.7\ \mu m$. In other words, the term K_d/ha in equation (2) shows a negligible influence on the calculation of K_c when the Ag particle size approaches 2.7 μm at 10% content. This indicates that the predicted curve in Fig. 5 without considering the term K_d/ha is a reasonable estimation. In fact, the use of $K_c = 39\ W/m \cdot K$ in equation (3) may readily involve both the pore phase and other defects such as interfacial fracture. The negligible contact resistance deduced for composite containing 10% Ag substantiates that the microcracking effect is negligible. The deviations which exists between the predicted values and the measured values as Ag ≥ 5% (Fig. 5) is due primarily to the pore phase.

Upon measuring the thermal diffusivity of the composites with a thermal cycling test, Figs 6(a) and (b) show that at 5% Ag, thermal diffusivity values are identical for both cycles [Fig. 6(a)], however, a small hysteresis loop is observed on return to room temperature at 10% Ag [Fig. 6(b)]. The true reason for

$$ha = \frac{K_d[K_m(2-2V_d) - K_c(2+V_d)]}{[K_m(2-2V_d) - K_c(2+V_d)] - K_d[(1+2V_d) - K_c/K_m(1-V_d)]} \tag{3}$$

$$a_c = \frac{1}{h}\frac{1}{P - 1/K_d} \tag{4}$$

and

$$P = \frac{1}{K_d}\left\{\frac{V_d\left[\left(\frac{K_c}{K_m}+2\right)\left(\frac{K_d}{K_m}-1\right)\right] + \left(1-\frac{K_c}{K_m}\right)\left(\frac{K_d}{K_m}+2\right)}{V_d\left(2+\frac{K_c}{K_m}\right) + 2\left(\frac{K_c}{K_m}-1\right)} + 1\right\}.$$

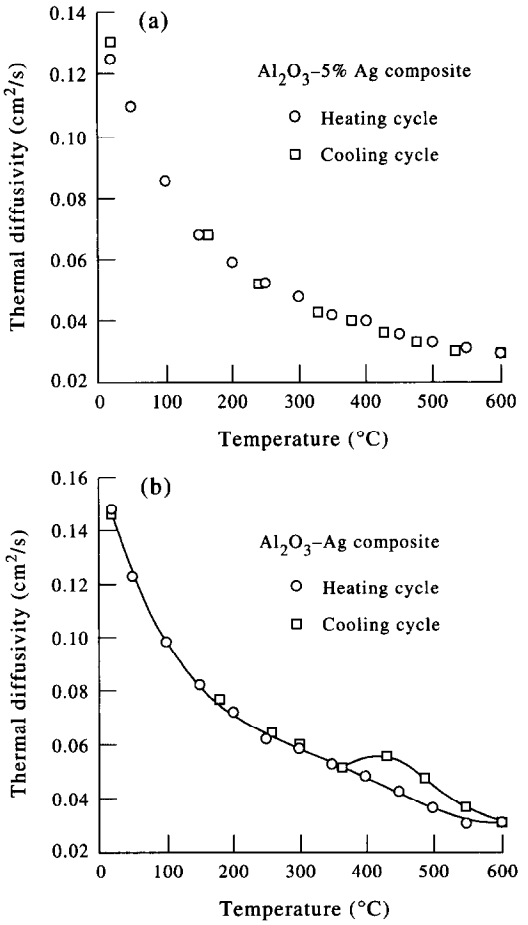

Fig. 6. Thermal cycling test made on the composite containing: (a) 5%; and (b) 10% Ag, which showed a hysteresis loop at 10 vol.% Ag.

such a hysteresis behavior is not quite clear at present. One explanation, which is based on the experimental observation in the $MgTi_2O_5$ ceramic by Siebeneck [28], might be referred to as the occurrence of internal microcracking during cooling. However, this appears to contradict the calculation of interfacial contact resistance presented earlier.

Therefore, one plausible explanation is proposed, which is assumed to result from the formation of cavity along the interface [29] once the local tensile stress becomes large (particularly for the larger Ag particles at 10% Ag) and exceeds the strength of the Al_2O_3–Ag interface. Since the heating cycle can be regarded as an annealing process, after which the internal stresses were partially relaxed. According to McKeown and Hudson [30], the ductility of Ag phase then would increase, accompanied with a decreased yield strength. Thus, a lower cooling temperature is usually required to yield sufficient stresses for activity formation, and this causes higher values of thermal diffusivity than the corresponding heating portion of the curve [Fig. 6(b)], constructing the hysteresis effect. This cavity phase, acting as porosity, reduces composite conductivity but does not suppose to enhance the interfacial contact resistance which has been verified by previous calculation. Therefore, the cavity formation appears to provide a more reasonable explanation for such a hysteresis phenomenon. The absence of the hysteresis loop in the composite with 5% Ag is probable due to the fact that the internal stresses are too low to have any important effect on the formation of cavity along the Al_2O_3–Ag interface.

4. CONCLUSIONS

The microstructure and the thermal conduction properties of Al_2O_3–Ag composites were investigated. The Ag inclusions distributed randomly throughout the matrix phase rather than forming a thin metal foil within the Al_2O_3 matrix. Interfacial thermal conductance h is determined to be 4.1×10^8 W/m·K and a corresponding critical Ag particle size of $\sim 2.7\ \mu$m is attained. Above the critical diameter (D_c) the composite conductivity can be evaluated accurately by using Hasselman–Johnson equation [equation (2)] without further considering the influence of interfacial contact resistance, i.e. original Maxwell–Rayleigh equation. The lower thermal conductivity of the composites containing 5% Ag compared to that of theoretical prediction is primarily due to the residual pore phase, and associates with cavity formation at 10% Ag.

Acknowledgements—The authors gratefully acknowledge the National Council of Science for funding toward this research.

REFERENCES

1. C. O. McHugh, T. J. Whalen and M. Humenik Jr, *J. Am. Ceram. Soc.* **49,** 486 (1966).
2. Y. Nivas and R. M. Fulrath, *J. Am. Ceram. Soc.* **53,** 188 (1970).
3. V. V. Krstic, P. S. Nicholson and R. G. Hoagland, *J. Am. Ceram. Soc.* **64,** 499 (1981).
4. P. Hing and G. W. Groves, *J. Mater. Sci.* **7,** 427 (1972).
5. M. F. Ashby, F. J. Blunt and M. Bannister, *Acta metall.* **37,** 1847 (1989).
6. B. Budiansky, J. C. Amaziga and A. G. Evans, *J. Mech. Phys. Solids* **36,** 167 (1988).
7. W. H. Tuan and R. J. Brook, *J. Europ. Ceram. Soc.* **6,** 31 (1990).
8. C. S. Morgan, A. J. Moorlead and R. J. Lauf, *Am. Ceram. Soc. Bull.* **61,** 974 (1982).
9. B. R. Powell Jr, G. E. Youngblood, D. P. H. Hasselman and L. D. Bentsen, *J. Am. Ceram. Soc.* **63,** 581 (1980).
10. D. P. H. Hasselman and L. D. Bentsen, *J. Thermal Insulation* **6,** 91 (1982).
11. D. M. Liu, *Mater. Chem. Phys.* **36,** 350 (1994).
12. D. M. Liu, C. J. Chen and L. J. Lin, *J. appl. Phys.* **75,** 3765 (1994).
13. C. S. Morgan, *Thin Solid Films* **39,** 305 (1976).
14. R. W. Davidge and T. J. Green, *J. Mater. Sci.* **3,** 629 (1968).
15. J. Selsing, *J. Am. Ceram. Soc.* **44,** 419 (1961).
16. D. M. Liu, *J. Mater. Sci.* submitted.
17. W. Hume-Rothery and P. W. Keynolds, *Proc. R. Soc.* **A167,** 25 (1938).
18. *Metal Handbook*, 8th edn, Vol. 1. Properties and Selection of Metals (edited by T. Lyman), Am. Soc. Metals, Metals Park, Novelty, Ohio (1961).

19. W. H. Tuan and W. R. Chen, *J. Europ. Ceram. Soc.* **14,** 37 (1994).
20. D. P. H. Hasselman and L. F. Johnson, *J. Composite Mater.* **21,** 508 (1987).
21. L. Raileigh, *Phil. Mag.* **34,** 481 (1892).
22. J. C. Maxwell, *A Treatise on Electricity and Magnetism*, 3rd edn. Oxford Univ. Press, Oxford (1904).
23. A. Eucken, *Ann. Physik* **34,** 185 (1911).
24. D. P. H. Hasselman, K. Y. Donaldson and A. L. Geiger, *J. Am. Ceram. Soc.* **75,** 3137 (1992).
25. Y. Benveniste and T. Miloh, *Int. J. Engng Sci.* **24,** 1537 (1986).
26. A. G. Every, Y. Tzon, D. P. H. Hasselman and R. Raj, *Acta metall. mater.* **40,** 123 (1992).
27. D. M. Liu, *Phil. Mag.* Submitted.
28. H. J. Siebeneck, D. P. H. Hasselman, J. J. Cleveland and R. C. Bradt, *J. Am. Ceram. Soc.* **60,** 336 (1977).
29. F. A. McClintock, *On the Mechanics of Fracture from Inclusion*, p. 255 in Ductility. Am. Soc. Metals (1967).
30. J. McKeown and O. Hudson, *J. Inst. Metal.* **60,** 109 (1937).